

PlanGen: Towards Unified Layout Planning and Image Generation in Auto-Regressive Vision Language Models

Runze He Bo cheng Yuhang Ma Qingxiang Jia Shanyuan Liu
 Ao Ma Xiaoyu Wu Liebucha Wu Dawei Leng[†] Yuhui Yin
 360 AI Research
 herunze8265@gmail.com, {chengbol, lengdawei}@360.cn

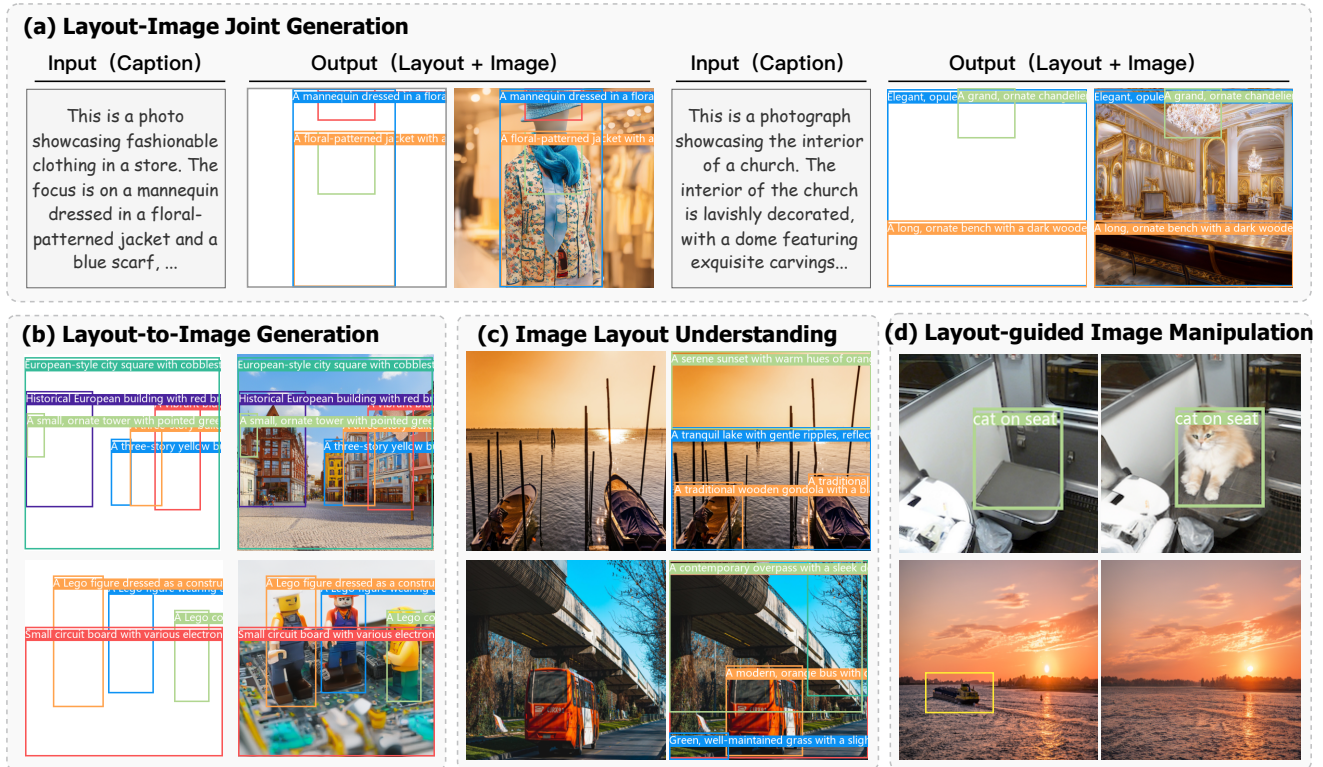


Figure 1. PlanGen models **layout planning** and **image generation** jointly, allowing layout planning before generating corresponding images, and the two processes are completed in a unified model. PlanGen can perform multi-type tasks related to layout, including **a)** layout-image joint generation, **b)** layout-to-image generation, **c)** image layout understanding and **d)** layout-guided image manipulation.

Abstract

In this paper, we propose a unified layout planning and image generation model, PlanGen, which can pre-plan spatial layout conditions before generating images. Unlike previous diffusion-based models that treat layout planning and layout-to-image as two separate models, PlanGen jointly models the two tasks into one autoregressive transformer using only next-token prediction. PlanGen integrates lay-

out conditions into the model as context without requiring specialized encoding of local captions and bounding box coordinates, which provides significant advantages over the previous embed-and-pool operations on layout conditions, particularly when dealing with complex layouts. Unified prompting allows PlanGen to perform multitasking training related to layout, including layout planning, layout-to-image generation, image layout understanding, etc. In addition, PlanGen can be seamlessly expanded to layout-guided image manipulation thanks to the well-designed modeling, with teacher-forcing content manipulation pol-

[†]Corresponding authors.

icy and negative layout guidance. Extensive experiments verify the effectiveness of our PlanGen in multiple layout-related tasks, showing its great potential. Code is available at: <https://360cvgroup.github.io/PlanGen>.

1. Introduction

In recent years, the field of image synthesis has received widespread attention from the community, and technologies such as GAN [20, 30, 70], autoregressive image generation [23, 35, 54, 59], and diffusion models [27, 53] have made great progress. Among them, diffusion models dominate because of their more stable training, sampling diversity, and high quality. Recently, autoregressive image generation has been widely explored because of its scalability and compatibility with large language models (LLMs).

With the continuous advancement of text-to-image foundation models [5, 44, 49, 51], their applications in commercial scenarios have become increasingly diverse. While fundamental text-to-image models primarily focus on text-image alignment, users often have more specific requirements regarding the spatial arrangement and interactions between objects. As shown in Figure 2, recent diffusion-based methods [12, 36, 62, 71, 76] introduce layout conditions into the image generation process. Despite the promising results, it faces two shortcomings: 1) Inability to expand to layout-image joint generation, which leads to reliance on another layout planning model. 2) Suboptimal encoding of layout condition, which is mainly caused by embed-and-pool operation on local captions to unify layout conditions for facilitating model training.

We propose an autoregressive visual-language model, PlanGen, which can complete layout planning and layout-to-image generation in a unified model. Just like thinking about what object each area should be before generating an image, such an explicit planning process allows the model to enjoy more powerful image generation capabilities. PlanGen takes layout conditions as context input, with extremely strong flexibility and scalability, no need to compress the layout conditions as previous methods [36, 62, 71, 76], allowing as detailed and complex local descriptions as possible, leading to a more aligned layout-to-image generation thanks to transformer’s long context dependencies. PlanGen allows multi-task training related to layout through unified prompting, including layout planning, layout-to-image generation, and image layout understanding. Additionally, through teacher-forcing content manipulation and negative layout guidance, PlanGen can be extended to layout-guided image manipulation without specialized training.

Our contributions are summarized as follows: (1) We present the first layout-image joint generation model based on the autoregressive vision-language model. (2) We pro-

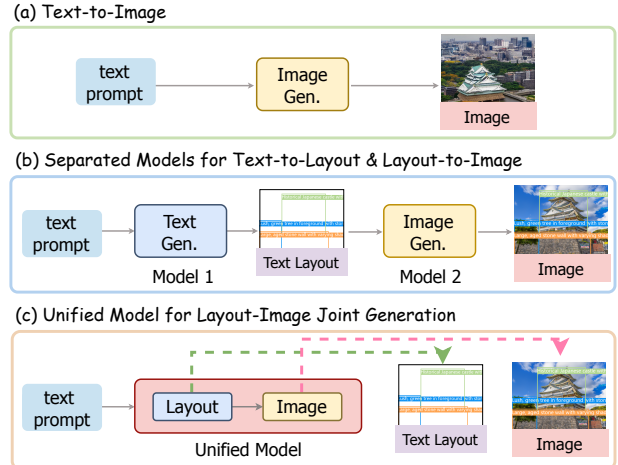


Figure 2. Different paradigms of image generation. **a)** The naive text-to-image cannot control the layout of the generated images. **b)** Previous methods use two independent models to complete layout planning and image generation. **c)** We adopt a unified model to complete layout planning and image generation.

pose a unified prompting paradigm to allow layout-image joint modeling, as well as multitasking training related to layout conditions. (3) We further extend PlanGen to layout-guided image manipulation through teacher-forcing content manipulation and negative layout guidance.

2. Related Works

Vision-Language Models (VLMs) In recent years, large vision-language models [1, 2, 7, 29, 40] have made remarkable breakthroughs. As a critical research direction, unified model with understanding and vision generation abilities [11, 15, 19, 58, 63, 65, 67, 73, 75] is being widely explored. Early approach SEED-X [19] applies another independent diffusion model to complete the visual generation task. Show-o [67] performs autoregressive and discrete diffusion modeling in one transformer. Transfusion [75] and MonoFormer [73] integrate the diffusion process into next-token prediction. Emu3 [63], Janus [65] as well as Janus-Pro [11] only use next-token prediction in training and also achieve promising results.

Autoregressive Image Generation Autoregressive image generation models [23, 35, 54, 56, 57, 59] have recently received widespread attention from the community due to their scalability and compatibility with LLMs. LlamaGen [54] apply the original “next-token prediction” paradigm of LLMs to the visual generation domain. MaskGIT [9] introduces a bidirectional transformer decoder and predicts randomly masked tokens by attending to tokens in all directions, instead of decoding images sequentially following the raster scan ordering. VAR [59] redefines the autoregressive image generation as a coarse-to-fine process, i.e. “next-scale prediction”, showing promising results.

MAR [35] performs autoregressive image generation in a continuous-valued space, with additional diffusion MLPs to model the per-token probability distribution.

Layout-to-Image Generation The layout-to-image generation methods can generally be categorized into training-free [10, 66] and training-based [12, 17, 22, 36, 45, 62, 71, 76] approaches. Early methods, such as CAG [10], which do not require training, laid the foundation for the field. Recent research, however, has primarily focused on training-based approaches. For instance, GLIGEN [36] explored specialized attention mechanisms, while HiCo [12] investigated methods for controlling the introduction of conditions, which can be used seamlessly as plugins. Furthermore, the introduction of CreatiLayout [71] in MM-DiT [14, 34] has further advanced controllable image generation based on layout design.

Image Manipulation The huge advances in image generation have also promoted research on image manipulation, i.e. image editing. The task is also dominated by diffusion-based models. Early training-free methods [8, 25, 41, 60], such as Prompt-to-Prompt [25], complete the image editing process by manipulating attention mechanisms. To edit real images, it is also necessary to inversion the real images, and the editing effect is not ideal. Some methods [3, 13, 42, 43] have been proposed to achieve diversified editing like object dragging. Instruction-based methods [6, 18, 24, 28, 72, 74] represented by Instruct-Pix2Pix [6] use natural language instructions to complete image editing, which relies on training on large-scale instruction editing datasets.

3. Methods

3.1. Overview

As shown in Figure 3, PlanGen based on the architecture of the autoregressive vision language model, supports layout-image joint generation in one transformer with causal attention. Given a text prompt T by the user, instead of directly generating the image, PlanGen performs spatial layout planning first to obtain the layout condition C , which imagines the desired position of each subject in the text prompt, and then completes the image generation process under the condition of both text prompt T and planned layout C .

3.2. Joint Generation Modeling

3.2.1. Unified Prompting

As shown in Figure 4a, the layout planning and image synthesis of PlanGen are performed in sequence during the same round of inference. We use newly inserted special tokens `<grounding>` and `</grounding>` to mark the beginning and the end of the layout condition. After the layout condition is planned, we use `<image.start>` to trigger the image generation process.

To help the model understand the layout condition, as

shown in Figure 4b, we use `<ref>` and `</ref>` to wrap local descriptions like Qwen [4]. Each local description corresponds to a bounding box coordinate list, which is placed between `<box>` and `</box>`. The coordinate list contains four integers standardized to 0-1000, representing the upper left corner and the lower right corner of the bounding box.

Thanks to the flexible context length in autoregressive models, local descriptions in PlanGen can be as detailed as needed, in contrast to the previous diffusion-based methods [36, 62, 71, 76] which need to perform pooling or truncation operations to reduce and unify the length of the local description embeddings. In addition, due to the parallel training advantages of autoregressive transformers, layout planning and layout-to-image generation can perform training in the same batch.

3.2.2. Image Layout Understanding Learning

The ability to understand the layout of real images can help the model generate images that are more in line with the layout conditions, intuitively, because this can further strengthen the model’s in-depth understanding of the relationship between layout conditions and corresponding images. In addition, including the task of image layout understanding to PlanGen can move further towards a more general layout VLM.

Given an image I , we expect PlanGen to be able to analyze its layout conditions. Specifically, we first extract high-dimensional image features from I using SigLIP [69] encoder, then flatten and map them into the text feature space, following Janus-Pro [11]. The prompt paradigm of image layout understanding is illustrated in Figure 4c. In order to reduce the difficulty of directly predicting the layout conditions, we predict the caption first before predicting the layout conditions.

3.2.3. Training Objectives

The training of all tasks in PlanGen is based on next-token prediction. We assume a sequence with M text prompt tokens $\mathbf{t} = \{t_1, t_2, \dots, t_M\}$, N layout tokens $\mathbf{l} = \{l_1, l_2, \dots, l_N\}$, X image tokens to be generated $\mathbf{g} = \{g_1, g_2, \dots, g_X\}$. Without loss of generality, we introduce layout planning and layout-to-image generation that can be trained in parallel separately.

Layout Planning We maximize the likelihood of layout tokens given text prompt tokens and all previously generated layout tokens by employing the standard language modeling objective:

$$\mathcal{L}_{LP} = \sum_i \log p_{\theta}(l_i | \mathbf{t}, l_{<i>i</i>}), \quad (1)$$

where p indicates the conditional probability of PlanGen, parameterized by weights θ .

Layout-to-Image Generation Similarly, we maximize the likelihood of image tokens given text prompt tokens, layout

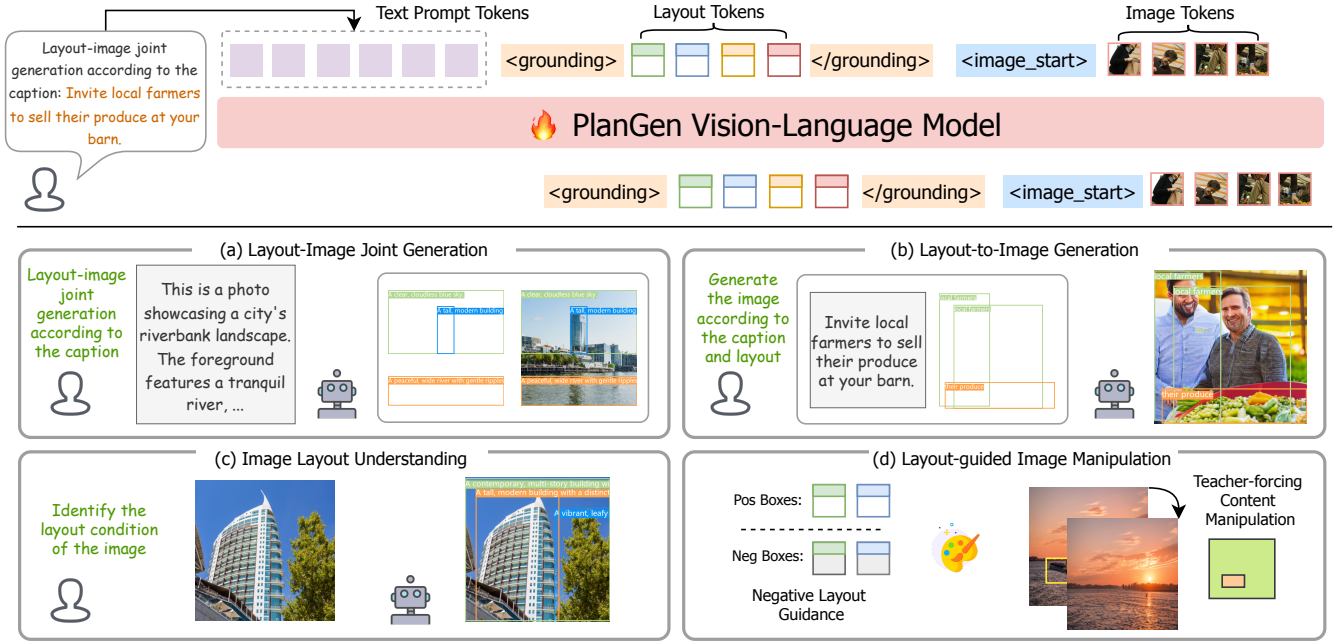


Figure 3. **Upper:** PlanGen models layout planning and image generation jointly in an autoregressive visual-language model through a unified prompting design with the next-token prediction training objective. **Lower:** Illustration of PlanGen’s multitasking related to layout: **a)** layout-image joint generation, **b)** layout to image generation, **c)** image layout understanding and **d)** layout-guided image manipulation.

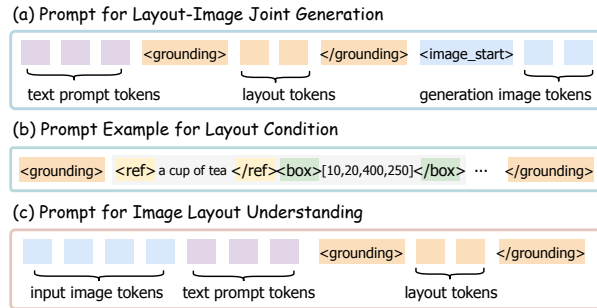


Figure 4. Prompt design of PlanGen. **a)** Prompt for Layout-Image Joint Generation. **b)** Prompt Example for Layout Condition. **c)** Prompt for Image Layout Understanding.

tokens, and previously generated image tokens, as formulated below:

$$\mathcal{L}_{LIG} = \sum_i \log p_{\theta}(\mathbf{g}_i | \mathbf{t}, \mathbf{l}, \mathbf{g}_{<i}) \quad (2)$$

Image Layout Understanding The task requires the introduction of K conditional image tokens $\mathbf{q} = \{\mathbf{q}_1, \mathbf{q}_2, \dots, \mathbf{q}_K\}$. We maximize the likelihood of layout tokens as follows:

$$\mathcal{L}_{ILU} = \sum_i \log p_{\theta}(\mathbf{l}_i | \mathbf{q}, \mathbf{t}, \mathbf{l}_{<i}) \quad (3)$$

The total training loss is summarized as follows:

$$\mathcal{L} = \alpha \mathcal{L}_{LP} + \beta \mathcal{L}_{LIG} + \gamma \mathcal{L}_{ILU}, \quad (4)$$

where α, β, γ are the hyperparameters to balance different losses, which are all set to 1 empirically in our experiments.

3.3. Layout-guided Image Manipulation

Benefiting from the modeling paradigm defined by layout conditions, PlanGen could control the generation of the contents of the local area based on the corresponding local captions and bounding boxes, which allows us to easily extend PlanGen to layout-guided image manipulation without further task-specific training.

3.3.1. Teacher-forcing Content Manipulate

One difficulty in image manipulation is to keep non-edited areas unchanged, and previous diffusion model-based approaches often require targeted training or inverse processes to achieve this goal, as its implicit features are difficult to manipulate directly. In the paradigm of autoregressive image modeling, we can achieve this through teacher-forcing.

Specifically, we can pre-calculate token position set \mathcal{P}_{edit} based on the bounding boxes to be edited. For tokens within \mathcal{P}_{edit} that require editing, we perform layout-to-image token sampling \mathcal{F} , or else we directly select pre-calculated tokens at corresponding mapped positions. The prediction process of the i -th image token e_i is defined as follows:

Dataset	Layout Planning	Layout-to-Image Gen.	Image Layout Und.	# Samples
HiCo [12]	✓	✓	✓	1,250,466
LayoutSAM [71]	✓	✓	✓	2,665,509
OpenImage [33]	✓	✓	✓	1,743,042
LayoutGPT [16]	✓	✗	✗	40,481

Table 1. **Statistics of datasets** used for training.

$$\mathbf{e}_i = \begin{cases} \mathcal{F}(\mathbf{t}, \mathbf{l}, \mathbf{e}_{<i}, i) & \text{if } i \in \mathcal{P}_{\text{edit}}, \\ \mathcal{M}(i, \mathbf{o}) & \text{if } i \notin \mathcal{P}_{\text{edit}}, \end{cases} \quad (5)$$

where \mathbf{o} represents the image tokens of the original image, and \mathcal{M} maps the i -token to corresponding image token in \mathbf{o} .

3.3.2. Negative Layout Guidance

To further improve editing quality, we propose negative layout guidance to unlock the huge potential of layout-based image manipulation methods. Existing methods often struggle to solve the artifacts after object deletion, as previous methods [55, 64] have pointed out.

Thanks to our token-based layout conditions, we can easily incorporate negative layout guidance into the classifier-free guidance to suppress the generation of artifacts without causing additional inference overhead.

$$\tilde{e}_\theta(\mathbf{t}, \mathbf{l}, \mathbf{g}_{<i}) = e_\theta(\tilde{\mathbf{t}}, \tilde{\mathbf{l}}, \mathbf{g}_{<i}) + s \cdot (e_\theta(\mathbf{t}, \mathbf{l}, \mathbf{g}_{<i}) - e_\theta(\tilde{\mathbf{t}}, \tilde{\mathbf{l}}, \mathbf{g}_{<i})), \quad (6)$$

where e_θ and \tilde{e}_θ indicates predicted logits and modulated final logits, $\tilde{\mathbf{t}}$ and $\tilde{\mathbf{l}}$ are negative text prompt tokens and negative layout tokens respectively. The guidance scale s is set to 5.

4. Experiments

4.1. Training Datasets

As shown in Table 1, we use two existing large-scale layout-to-image datasets in training, including HiCo [12] derived from GRIT-20M [47] and LayoutSAM [71] derived from SAM [31]. In addition, we also introduce OpenImage V6 [33] dataset. We apply MiniCPM [46] to caption the images and use object class names as local captions, which complements the long local captions in HiCo and LayoutSAM. Furthermore, considering that these three datasets focus on complex prompts and layouts, we also introduce pure planning data constructed by LayoutGPT [16].

4.2. Implementation Details

Our experiment is based on pre-trained Janus-Pro 1.5B [11]. The training batch sizes of layout-image joint training, image layout understanding, and pure layout planning are 3, 3, and 2 respectively. We train our PlanGen for 200,000 steps

on $8 \times 80\text{GB}$ NVIDIA A100 GPUs with AdamW [39] optimizer, and the learning rate is set to $5e-5$ with a total batch size of 64. Images are uniformly processed to 384×384 resolution.

4.3. Layout Planning

Settings. We compare PlanGen’s layout planning ability with existing powerful foundational LLMs: (1) Qwen2.5-7b-instruct [21] (2) Llama3.1-8b-instruct [40]. We use in-context learning to make LLMs generate layout conditions according to global captions. We conduct evaluations on PlanGen-1K benchmark, which is derived from LayoutSAM-Eval, used for multitasking evaluation related to layout. Considering that the layouting planning has a high degree of freedom, it is not reasonable to compare the results with ground truth layouts. Following [71], we use PlanGen to perform layout-to-image generation for layouts predicted by different methods and indirectly judge the quality of the layout by judging the quality of generated images. We calculate (1) PickScore, which derives from the preference predictor, (2) CLIPScore, which measures the CLIP [48] image-text similarity between the generated images and corresponding text prompts, (3) FID [26] and (4) Inception Score (IS) [52].

Results. As shown in Figure 5, PlanGen can generate reasonable layouts from complex global captions. Compared with Qwen2.5-7b-instruct and Llama3.1-8b-instruct, the local descriptions of bounding boxes generated by PlanGen are more detailed and specific, which promotes the consistency of the generation results with the global captions. Furthermore, the planned layouts enjoy more reasonable spatial relations, resulting in better image quality. The quantitative analysis in Table 3 also confirms the advantage of PlanGen in layout planning. Compared with the other two LLMs, the image results generated based on PlanGen’s layout predictions have lower FID and are even close to the results generated by using ground-truth layout conditions.

4.4. Layout-to-Image Generation

Settings. Layout-to-image generation was dominated by diffusion-based models. We evaluate PlanGen’s ability of layout-to-image with (1) GLIGEN [36] (2) Ranni [17] (3) MIGC [76] (4) InstanceDiff [62] (5) HiCo [12] and (6) Creatilayout [71]. PlanGen is the only layout-to-image model based on the autoregression paradigm. We conduct evaluations on LayoutSAM-Eval benchmark following [71] and report region-wise quality and global-wise quality. The region-wise quality includes spatial, color, texture, and shape scores obtained from MiniCPM [46], while the global-wise quality includes traditional indicators like FID, IS, and so on. More details can be found in [71].

Results. As shown in Figure 6, PlanGen could generate corresponding images based on given layout conditions, and

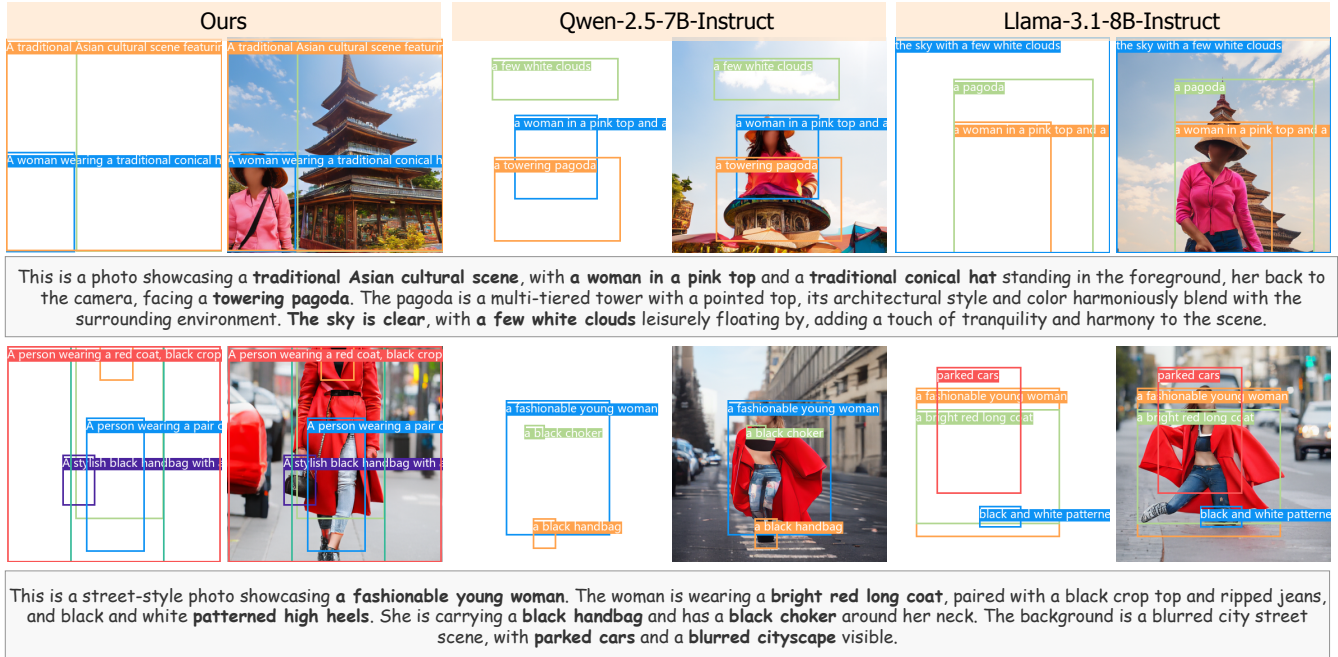


Figure 5. Examples for layout planning. Compared with Qwen-2.5-7b-instruct [21] and Llama-3.1-8b-instruct [40], PlanGen generates more reasonable layout conditions from complex global captions. We use PlanGen to conduct layout-to-image generation for the layout conditions generated by the three methods to further observe the quality of the layout conditions.

Type	Method	Region-wise Quality				Global-wise Quality				
		Spatial \uparrow	Color \uparrow	Texture \uparrow	Shape \uparrow	IR \uparrow [68]	Pick \uparrow [32]	CLIP \uparrow	FID \downarrow	IS \uparrow
	Real Images	98.95	98.45	98.90	98.80	-	-	-	-	-
Diffusion	GLIGEN [36]	77.53	49.41	55.29	52.72	-10.31	20.78	32.42	21.92	20.57
	Ranni [17]	41.38	24.10	25.57	23.35	-28.46	20.49	31.40	27.24	19.81
	MIGC [76]	85.66	66.97	71.24	69.06	-13.72	20.71	31.36	21.19	19.65
	InstanceDiff [62]	87.99	69.16	72.78	71.08	9.14	21.01	31.40	19.67	20.02
	HiCo [12]	90.22	69.89	73.95	72.75	<u>42.87</u>	22.44	<u>33.11</u>	19.30	22.50
	CreatiLayout [71]	92.67	<u>74.45</u>	<u>77.21</u>	<u>75.93</u>	69.47	<u>22.02</u>	34.01	<u>19.10</u>	<u>22.04</u>
AR	PlanGen	<u>92.21</u>	82.69	86.53	85.36	39.58	21.43	31.96	13.91	19.31

Table 2. Layout-to-image quantitative comparison on the LayoutSAM-Eval. Only PlanGen is based on the autoregressive paradigm.

Method	Pick \uparrow	CLIP \uparrow	FID \downarrow	IS \uparrow
GT Layout	21.44	31.91	48.67	13.97
Qwen2.5-7b-it [21]	20.92	31.47	472.38	13.44
Llama3.1-8b-it [40]	21.01	31.64	464.07	13.77
PlanGen	21.42	31.93	50.73	15.44

Table 3. Layout planning quantitative comparison of PlanGen with Qwen2.5-7b-instruct [21] and Llama3.1-8b-instruct [40] on PlanGen-1K.

the generated results show a high degree of consistency with the layout conditions. In the 1st row, only PlanGen gener-

ates a reasonable “ancient stone castle”. Although CreatiLayout has a higher image aesthetics and realism, it produces a result of the separation of the upper and lower parts of the image, which is not harmonious. We observe that the results generated by InstanceDiff lack sufficient realism and tend toward animation style. GLIGEN will ignore certain layout information in some cases, such as the 2nd row, missing “clean blue water”. PlanGen is generally capable of generating realistic images and meeting layout conditions. However, it shows limitations in generating human figures, as evidenced in the last row. This is consistent with the quantitative results in Table 2, PlanGen performs well



Figure 6. Qualitative comparisons of PlanGen with other baselines on layout-to-image generation task, including GLIGEN [36], InstanceDiff [62], and CreatiLayout [71]. PlanGen generates realistic images that meet the layout conditions, which has obvious advantages compared to previous diffusion-based methods.

in region-wise quality and significantly exceeds previous diffusion-based methods, thanks to its strong understanding of the layout context. In addition, the FID metric of PlanGen also leads other methods, verifying its excellent image generation quality.

4.5. Image Layout Understanding

Settings. Image layout understanding has similarity to grounding detection to some extent, both to obtain local captions and corresponding bounding box coordinates, but image layout understanding does not aim at detecting objects in the figure as its ultimate goal. We compare PlanGen’s image layout understanding ability with specialized grounding detection model (1) Grounding-DINO [38] and LLMs with grounding capability (2) Qwen-VL-Chat [4] (3) CogVLM-grounding [61]. We conduct the evaluation on our PlanGen-1K benchmark, reporting AP, AP50, AP75, and AR. Additional details are provided in the supplemental material.

Method	AP \uparrow	AP50 \uparrow	AP75 \uparrow	AR \uparrow
Grounding-DINO [38]	50.00	61.66	54.92	69.34
Qwen-VL-Chat [4]	5.16	9.17	5.82	20.64
CogVLM-grounding [61]	9.05	13.03	9.95	29.27
PlanGen	33.48	44.76	36.71	50.98

Table 4. Image layout understanding quantitative comparison of PlanGen with Grounding-DINO [38], Qwen-VL-Chat [4] and CogVLM-grounding [61] on PlanGen-1K.

Results. As shown in Table 4, compared with Qwen-VL-Chat and CogVLM-grounding, PlanGen, specially trained in image layout understanding, achieves excellent layout understanding capabilities with higher AP and AR metrics. It should be noted that PlanGen can even be close to the performance of Grounding-DINO, which is often a specialized tool for data annotation, showing PlanGen’s promising prospects.

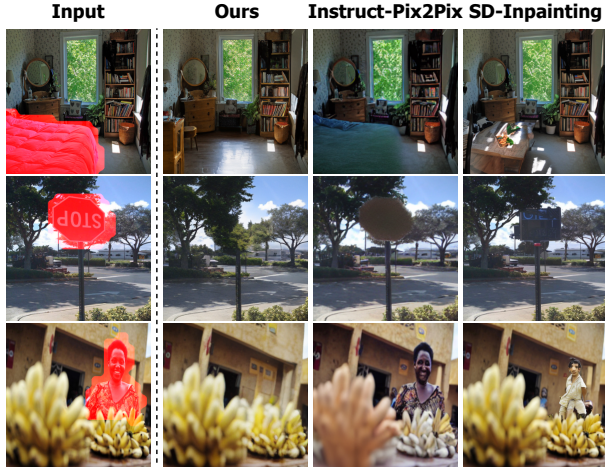


Figure 7. Qualitative comparisons of PlanGen with Instruct-Pix2Pix [6] and SD-Inpainting [50] on the object removal task. The red areas of images in the 1st column are the objects to be deleted.

4.6. Image Manipulation

Settings. In this part, we focus on comparing the object deletion ability of PlanGen. We choose two classic diffusion-based baselines: (1) Instruct-Pix2Pix [6] (2) SD-Inpainting [50], which is specially trained inpainting model, because it is difficult to manipulate the latent directly in the diffusion model, while PlanGen could conduct image generation and editing in one unified model. We report the following indicators in 200 object removal cases derived from COCO [37] test set, including (1) Success Rate (SR), we calculate it by asking the visual language model MiniCPM [46] whether there are objects to be deleted in targeted area. (2) LocalCLIP, which measures the deletion ability by evaluating the image-text similarity of the local image areas and the corresponding local descriptions. (3) IS, which measures the quality of the image.

Results. As shown in Figure 7, PlanGen has more obvious advantages when deleting objects, and can more thoroughly delete objects in local areas, making it less likely to leave artifacts or cause image quality to decline. This is consistent with the results in Table 5, and PlanGen achieves the highest deletion success rate. As illustrated in the first row of Figure 7, when the bed is removed, PlanGen also generates a light reflection on the floor originating from the window. Instruct-Pix2Pix often causes most of the entire image to change, and it is often impossible to completely delete. SD-Inpainting is prone to leaving artifacts in the area to be deleted, affecting the quality of the image. Additional image manipulation examples for more editing types are provided in the supplemental material.

Method	SR \uparrow	LocalCLIP \downarrow	IS \uparrow
Instruct-Pix2Pix [6]	40.00	23.65	9.20
SD-Inpainting [50]	66.50	22.61	7.73
PlanGen	<u>77.50</u>	<u>21.96</u>	<u>8.45</u>
+Neg. Layout Guidance	86.50	21.90	8.43

Table 5. Object removal quantitative comparison of PlanGen with Instruct-Pix2Pix [6] and SD-Inpainting [50].

LIG	LP	ILU	Enc	Spatial \uparrow	Color \uparrow	Texture \uparrow	Shape \uparrow
\checkmark	\times	\times	N	87.19	72.25	77.18	76.35
\checkmark	\times	\times	N	83.25	69.46	73.73	70.28
\checkmark	\checkmark	\checkmark	N	87.52	68.14	74.55	<u>71.26</u>
\checkmark	\checkmark	\checkmark	S	81.94	59.61	67.65	66.34

Table 6. Ablation studies about the task types used in PlanGen’s training and the encoding type of numerical values (Enc). “LIG” stands for Layout-to-Image Generation, “LP” for Layout Planning, and “ILU” for Image Layout Understanding. “S” refers to encoding numerical values into special tokens, whereas “N” means treating numerical values as normal text.

4.7. Ablation Study

In Table 6, we perform a series of ablation experiments on a subset of the training dataset. we compare the different encoding types of numerical values and find that PlanGen can achieve better results by directly considering the values as texts rather than encoding them into special tokens. In addition, we also ablate the impact of different tasks adopted in the experiment. The introduction of image layout understanding can improve the effect of the model. The model trained with all tasks has a similar effect as the model trained with layout-to-image task alone, which verifies the effectiveness of PlanGen using multi-task training. In addition, in Table 5, we ablate the impact of whether negative layout guidance is used on the object deletion task. By introducing this strategy, we observe that the deletion success rate has been greatly improved.

5. Discussion

In this work, we demonstrate a unified model that integrates layout planning and layout-to-image generation into an autoregressive vision-language model, which also has the ability to understand the layout of real images. It performs well in layout planning, layout-to-image, and image layout understanding tasks, showing the great potential of a unified model. In addition, it can be expanded into image manipulation without further training with teacher-forcing content manipulation and negative layout guidance.

While promising, our work still faces several challenges, firstly, our experiments are trained on image resolution of 384×384 due to limited training resources. Experiments at

higher resolutions will help further improve the model’s effect. In addition, subsequent work can consider more advanced autoregressive image generation paradigms, including mask autoregressive generation [9] and next-scale prediction [59] paradigms.

References

- [1] Josh Achiam, Steven Adler, Sandhini Agarwal, Lama Ahmad, Ilge Akkaya, Florencia Leoni Aleman, Diogo Almeida, Janko Altmenschmidt, Sam Altman, Shyamal Anadkat, et al. Gpt-4 technical report. *arXiv preprint arXiv:2303.08774*, 2023. 2
- [2] Jean-Baptiste Alayrac, Jeff Donahue, Pauline Luc, Antoine Miech, Iain Barr, Yana Hasson, Karel Lenc, Arthur Mensch, Katie Millican, Malcolm Reynolds, Roman Ring, Eliza Rutherford, Serkan Cabi, Tengda Han, Zhitao Gong, Sina Samangooei, Marianne Monteiro, Jacob Menick, Sebastian Borgeaud, Andrew Brock, Aida Nematzadeh, Sahand Sharifzadeh, Mikolaj Binkowski, Ricardo Barreira, Oriol Vinyals, Andrew Zisserman, and Karen Simonyan. Flamingo: a visual language model for few-shot learning, 2022. 2
- [3] Omri Avrahami, Rinon Gal, Gal Chechik, Ohad Fried, Dani Lischinski, Arash Vahdat, and Weili Nie. Diffuhaul: A training-free method for object dragging in images. In *SIGGRAPH Asia 2024 Conference Papers*, pages 1–12, 2024. 3
- [4] Jinze Bai, Shuai Bai, Shusheng Yang, Shijie Wang, Sinan Tan, Peng Wang, Junyang Lin, Chang Zhou, and Jingren Zhou. Qwen-vl: A frontier large vision-language model with versatile abilities. *arXiv preprint arXiv:2308.12966*, 2023. 3, 7
- [5] James Betker, Gabriel Goh, Li Jing, Tim Brooks, Jianfeng Wang, Linjie Li, Long Ouyang, Juntang Zhuang, Joyce Lee, Yufei Guo, et al. Improving image generation with better captions. *Computer Science*. <https://cdn.openai.com/papers/dall-e-3.pdf>, 2023. 2
- [6] Tim Brooks, Aleksander Holynski, and Alexei A Efros. Instructpix2pix: Learning to follow image editing instructions. In *Proceedings of the IEEE/CVF Conference on Computer Vision and Pattern Recognition*, pages 18392–18402, 2023. 3, 8
- [7] Tom B. Brown, Benjamin Mann, Nick Ryder, Melanie Subbiah, Jared Kaplan, Prafulla Dhariwal, Arvind Neelakantan, Pranav Shyam, Girish Sastry, Amanda Askell, Sandhini Agarwal, Ariel Herbert-Voss, Gretchen Krueger, Tom Henighan, Rewon Child, Aditya Ramesh, Daniel M. Ziegler, Jeffrey Wu, Clemens Winter, Christopher Hesse, Mark Chen, Eric Sigler, Mateusz Litwin, Scott Gray, Benjamin Chess, Jack Clark, Christopher Berner, Sam McCandlish, Alec Radford, Ilya Sutskever, and Dario Amodei. Language models are few-shot learners. In *Advances in Neural Information Processing Systems 33: Annual Conference on Neural Information Processing Systems 2020, NeurIPS 2020, December 6-12, 2020, virtual*, 2020. 2
- [8] Mingdeng Cao, Xintao Wang, Zhongang Qi, Ying Shan, Xiao-hu Qie, and Yinqiang Zheng. Masactrl: Tuning-free mutual self-attention control for consistent image synthesis and editing. In *Proceedings of the IEEE/CVF International Conference on Computer Vision (ICCV)*, pages 22560–22570, 2023. 3
- [9] Huiwen Chang, Han Zhang, Lu Jiang, Ce Liu, and William T Freeman. Maskgit: Masked generative image transformer. In *Proceedings of the IEEE/CVF conference on computer vision and pattern recognition*, pages 11315–11325, 2022. 2, 9
- [10] Minghao Chen, Iro Laina, and Andrea Vedaldi. Training-free layout control with cross-attention guidance. In *Proceedings of the IEEE/CVF winter conference on applications of computer vision*, pages 5343–5353, 2024. 3
- [11] Xiaokang Chen, Zhiyu Wu, Xingchao Liu, Zizheng Pan, Wen Liu, Zhenda Xie, Xingkai Yu, and Chong Ruan. Januspro: Unified multimodal understanding and generation with data and model scaling. *arXiv preprint arXiv:2501.17811*, 2025. 2, 3, 5
- [12] Bo Cheng, Yuhang Ma, Liebuca Wu, Shanyuan Liu, Ao Ma, Xiaoyu Wu, Dawei Leng, and Yuhui Yin. Hico: Hierarchical controllable diffusion model for layout-to-image generation. *arXiv preprint arXiv:2410.14324*, 2024. 2, 3, 5, 6
- [13] Dave Epstein, Allan Jabri, Ben Poole, Alexei Efros, and Aleksander Holynski. Diffusion self-guidance for controllable image generation. *Advances in Neural Information Processing Systems*, 36:16222–16239, 2023. 3
- [14] Patrick Esser, Sumith Kulal, Andreas Blattmann, Rahim Entezari, Jonas Müller, Harry Saini, Yam Levi, Dominik Lorenz, Axel Sauer, Frederic Boesel, et al. Scaling rectified flow transformers for high-resolution image synthesis. *arXiv preprint arXiv:2403.03206*, 2024. 3
- [15] Rongyao Fang, Chengqi Duan, Kun Wang, Hao Li, Hao Tian, Xingyu Zeng, Rui Zhao, Jifeng Dai, Hongsheng Li, and Xihui Liu. Puma: Empowering unified mllm with multi-granular visual generation. *arXiv preprint arXiv:2410.13861*, 2024. 2
- [16] Weixi Feng, Wanrong Zhu, Tsu-jui Fu, Varun Jampani, Arjun Akula, Xuehai He, Sugato Basu, Xin Eric Wang, and William Yang Wang. Layoutgpt: Compositional visual planning and generation with large language models. In *NeurIPS*, 2023. 5
- [17] Yutong Feng, Biao Gong, Di Chen, Yujun Shen, Yu Liu, and Jingren Zhou. Ranni: Taming text-to-image diffusion for accurate instruction following. In *CVPR*, 2024. 3, 5, 6
- [18] Tsu-Jui Fu, Wenze Hu, Xianzhi Du, William Yang Wang, Yinfei Yang, and Zhe Gan. Guiding instruction-based image editing via multimodal large language models. *arXiv preprint arXiv:2309.17102*, 2023. 3
- [19] Yuying Ge, Sijie Zhao, Jinguo Zhu, Yixiao Ge, Kun Yi, Lin Song, Chen Li, Xiaohan Ding, and Ying Shan. Seed-x: Multimodal models with unified multi-granularity comprehension and generation. *arXiv preprint arXiv:2404.14396*, 2024. 2
- [20] Ian Goodfellow, Jean Pouget-Abadie, Mehdi Mirza, Bing Xu, David Warde-Farley, Sherjil Ozair, Aaron Courville, and Yoshua Bengio. Generative adversarial networks. *Communications of the ACM*, 63(11):139–144, 2020. 2

- [21] Alibaba Group. Qwen2.5-7b-it. <https://huggingface.co/Qwen/Qwen2.5-7B-Instruct>, 2024. 5, 6
- [22] Jiatao Gu, Ying Shen, Shuangfei Zhai, Yizhe Zhang, Navdeep Jaitly, and Joshua M Susskind. Kaleido diffusion: Improving conditional diffusion models with autoregressive latent modeling. *arXiv preprint arXiv:2405.21048*, 2024. 3
- [23] Jian Han, Jinlai Liu, Yi Jiang, Bin Yan, Yuqi Zhang, Zehuan Yuan, Bingyue Peng, and Xiaobing Liu. Infinity: Scaling bit-wise autoregressive modeling for high-resolution image synthesis, 2024. 2
- [24] Runze He, Kai Ma, Linjiang Huang, Shaofei Huang, Jialin Gao, Xiaoming Wei, Jiao Dai, Jizhong Han, and Si Liu. Freeedit: Mask-free reference-based image editing with multi-modal instruction, 2024. 3
- [25] Amir Hertz, Ron Mokady, Jay Tenenbaum, Kfir Aberman, Yael Pritch, and Daniel Cohen-Or. Prompt-to-prompt image editing with cross attention control. *CoRR*, abs/2208.01626, 2022. 3
- [26] Martin Heusel, Hubert Ramsauer, Thomas Unterthiner, Bernhard Nessler, and Sepp Hochreiter. Gans trained by a two time-scale update rule converge to a local nash equilibrium. In *NeurIPS*, 2017. 5
- [27] Jonathan Ho, Ajay Jain, and Pieter Abbeel. Denoising diffusion probabilistic models. In *NeurIPS*, 2020. 2
- [28] Yuzhou Huang, Liangbin Xie, Xintao Wang, Ziyang Yuan, Xiaodong Cun, Yixiao Ge, Jiantao Zhou, Chao Dong, Rui Huang, Ruimao Zhang, and Ying Shan. Smartedit: Exploring complex instruction-based image editing with multimodal large language models, 2023. 3
- [29] Binyuan Hui, Jian Yang, Zeyu Cui, Jiayi Yang, Dayiheng Liu, Lei Zhang, Tianyu Liu, Jiajun Zhang, Bowen Yu, Kai Dang, et al. Qwen2. 5-coder technical report. *arXiv preprint arXiv:2409.12186*, 2024. 2
- [30] Tero Karras, Samuli Laine, and Timo Aila. A style-based generator architecture for generative adversarial networks. In *Proceedings of the IEEE/CVF conference on computer vision and pattern recognition*, pages 4401–4410, 2019. 2
- [31] Alexander Kirillov, Eric Mintun, Nikhila Ravi, Hanzi Mao, Chloe Rolland, Laura Gustafson, Tete Xiao, Spencer Whitehead, Alexander C Berg, Wan-Yen Lo, et al. Segment anything. In *ICCV*, 2023. 5
- [32] Yuval Kirstain, Adam Polyak, Uriel Singer, Shahbuland Matiana, Joe Penna, and Omer Levy. Pick-a-pic: An open dataset of user preferences for text-to-image generation. *arXiv preprint arXiv:2305.01569*, 2023. 6
- [33] Alina Kuznetsova, Hassan Rom, Neil Alldrin, Jasper Uijlings, Ivan Krasin, Jordi Pont-Tuset, Shahab Kamali, Stefan Popov, Matteo Mallocci, Alexander Kolesnikov, et al. The open images dataset v4: Unified image classification, object detection, and visual relationship detection at scale. *International journal of computer vision*, 128(7):1956–1981, 2020. 5
- [34] Black Forest Labs. Flux. <https://blackforestlabs.ai/announcing-black-forest-labs>, 2024. 3
- [35] Tianhong Li, Yonglong Tian, He Li, Mingyang Deng, and Kaiming He. Autoregressive image generation without vector quantization. *Advances in Neural Information Processing Systems*, 37:56424–56445, 2025. 2, 3
- [36] Yuheng Li, Haotian Liu, Qingyang Wu, Fangzhou Mu, Jianwei Yang, Jianfeng Gao, Chunyuan Li, and Yong Jae Lee. Gligen: Open-set grounded text-to-image generation. In *CVPR*, 2023. 2, 3, 5, 6, 7
- [37] Tsung-Yi Lin, Michael Maire, Serge Belongie, James Hays, Pietro Perona, Deva Ramanan, Piotr Dollár, and C Lawrence Zitnick. Microsoft coco: Common objects in context. In *ECCV*, 2014. 8
- [38] Shilong Liu, Zhaoyang Zeng, Tianhe Ren, Feng Li, Hao Zhang, Jie Yang, Chunyuan Li, Jianwei Yang, Hang Su, Jun Zhu, et al. Grounding dino: Marrying dino with grounded pre-training for open-set object detection. *arXiv preprint arXiv:2303.05499*, 2023. 7
- [39] I Loshchilov. Decoupled weight decay regularization. *arXiv preprint arXiv:1711.05101*, 2017. 5
- [40] Meta. Llama-3.1-8b-instruct. <https://huggingface.co/meta-llama/Llama-3.1-8B-Instruct>, 2024. 2, 5, 6
- [41] Ron Mokady, Amir Hertz, Kfir Aberman, Yael Pritch, and Daniel Cohen-Or. Null-text inversion for editing real images using guided diffusion models. In *Proceedings of the IEEE/CVF Conference on Computer Vision and Pattern Recognition*, pages 6038–6047, 2023. 3
- [42] Chong Mou, Xintao Wang, Jiechong Song, Ying Shan, and Jian Zhang. Diffeditor: Boosting accuracy and flexibility on diffusion-based image editing. *arXiv preprint arXiv:2402.02583*, 2023. 3
- [43] Chong Mou, Xintao Wang, Jiechong Song, Ying Shan, and Jian Zhang. Dragondiffusion: Enabling drag-style manipulation on diffusion models. *arXiv preprint arXiv:2307.02421*, 2023. 3
- [44] Alex Nichol, Prafulla Dhariwal, Aditya Ramesh, Pranav Shyam, Pamela Mishkin, Bob McGrew, Ilya Sutskever, and Mark Chen. Glide: Towards photorealistic image generation and editing with text-guided diffusion models. *arXiv preprint arXiv:2112.10741*, 2021. 2
- [45] Weili Nie, Sifei Liu, Morteza Mardani, Chao Liu, Benjamin Eckart, and Arash Vahdat. Compositional text-to-image generation with dense blob representations. *arXiv preprint arXiv:2405.08246*, 2024. 3
- [46] OpenBMB. Minicpm-v-2.6. https://huggingface.co/openbmb/MiniCPM-V-2_6, 2024. 5, 8
- [47] Zhiliang Peng, Wenhui Wang, Li Dong, Yaru Hao, Shaohan Huang, Shuming Ma, and Furu Wei. Kosmos-2: Grounding multimodal large language models to the world. *arXiv preprint arXiv:2306.14824*, 2023. 5
- [48] Alec Radford, Jong Wook Kim, Chris Hallacy, Aditya Ramesh, Gabriel Goh, Sandhini Agarwal, Girish Sastry, Amanda Askell, Pamela Mishkin, Jack Clark, et al. Learning transferable visual models from natural language supervision. In *ICML*, 2021. 5
- [49] Aditya Ramesh, Prafulla Dhariwal, Alex Nichol, Casey Chu, and Mark Chen. Hierarchical text-conditional image gen-

- eration with clip latents. *arXiv preprint arXiv:2204.06125*, 2022. 2
- [50] Robin Rombach, Andreas Blattmann, Dominik Lorenz, Patrick Esser, and Björn Ommer. High-resolution image synthesis with latent diffusion models. In *CVPR*, 2022. 8
- [51] Chitwan Saharia, William Chan, Saurabh Saxena, Lala Li, Jay Whang, Emily L Denton, Kamyar Ghasemipour, Raphael Gontijo Lopes, Burcu Karagol Ayan, Tim Salimans, et al. Photorealistic text-to-image diffusion models with deep language understanding. In *NeurIPS*, 2022. 2
- [52] Tim Salimans, Ian Goodfellow, Wojciech Zaremba, Vicki Cheung, Alec Radford, and Xi Chen. Improved techniques for training gans. In *NeurIPS*, 2016. 5
- [53] Jiaming Song, Chenlin Meng, and Stefano Ermon. Denoising diffusion implicit models. In *ICLR*, 2021. 2
- [54] Peize Sun, Yi Jiang, Shoufa Chen, Shilong Zhang, Bingyue Peng, Ping Luo, and Zehuan Yuan. Autoregressive model beats diffusion: Llama for scalable image generation. *arXiv preprint arXiv:2406.06525*, 2024. 2
- [55] Wenhao Sun, Benlei Cui, Jingqun Tang, and Xue-Mei Dong. Attentive eraser: Unleashing diffusion model’s object removal potential via self-attention redirection guidance. *arXiv preprint arXiv:2412.12974*, 2024. 5
- [56] Zeyi Sun, Ziyang Chu, Pan Zhang, Tong Wu, Xiaoyi Dong, Yuhang Zang, Yuanjun Xiong, Dahua Lin, and Jiaqi Wang. X-prompt: Towards universal in-context image generation in auto-regressive vision language foundation models, 2024. 2
- [57] Haotian Tang, Yecheng Wu, Shang Yang, Enze Xie, Junsong Chen, Junyu Chen, Zhuoyang Zhang, Han Cai, Yao Lu, and Song Han. Hart: Efficient visual generation with hybrid autoregressive transformer. *arXiv preprint*, 2024. 2
- [58] Chameleon Team. Chameleon: Mixed-modal early-fusion foundation models. *arXiv preprint arXiv:2405.09818*, 2024. 2
- [59] Keyu Tian, Yi Jiang, Zehuan Yuan, Bingyue Peng, and Liwei Wang. Visual autoregressive modeling: Scalable image generation via next-scale prediction. 2024. 2, 9
- [60] Narek Tumanyan, Michal Geyer, Shai Bagon, and Tali Dekel. Plug-and-play diffusion features for text-driven image-to-image translation. In *Proceedings of the IEEE/CVF Conference on Computer Vision and Pattern Recognition (CVPR)*, pages 1921–1930, 2023. 3
- [61] Weihang Wang, Qingsong Lv, Wenmeng Yu, Wenyi Hong, Ji Qi, Yan Wang, Junhui Ji, Zhuoyi Yang, Lei Zhao, Xixuan Song, Jiazheng Xu, Bin Xu, Juanzi Li, Yuxiao Dong, Ming Ding, and Jie Tang. Cogvlm: Visual expert for pretrained language models. 2023. 7
- [62] Xudong Wang, Trevor Darrell, Sai Saketh Rambhatla, Rohit Girdhar, and Ishan Misra. Instancediffusion: Instance-level control for image generation. In *CVPR*, 2024. 2, 3, 5, 6, 7
- [63] Xinlong Wang, Xiaosong Zhang, Zhengxiong Luo, Quan Sun, Yufeng Cui, Jinsheng Wang, Fan Zhang, Yueze Wang, Zhen Li, Qiyang Yu, et al. Emu3: Next-token prediction is all you need. *arXiv preprint arXiv:2409.18869*, 2024. 2
- [64] Daniel Winter, Matan Cohen, Shlomi Fruchter, Yael Pritch, Alex Rav-Acha, and Yedid Hoshen. Objectdrop: Bootstrapping counterfactuals for photorealistic object removal and insertion. In *European Conference on Computer Vision*, pages 112–129. Springer, 2024. 5
- [65] Chengyue Wu, Xiaokang Chen, Zhiyu Wu, Yiyang Ma, Xingchao Liu, Zizheng Pan, Wen Liu, Zhenda Xie, Xingkai Yu, Chong Ruan, et al. Janus: Decoupling visual encoding for unified multimodal understanding and generation. *arXiv preprint arXiv:2410.13848*, 2024. 2
- [66] Jinheng Xie, Yuexiang Li, Yawen Huang, Haozhe Liu, Wentian Zhang, Yefeng Zheng, and Mike Zheng Shou. Boxdiff: Text-to-image synthesis with training-free box-constrained diffusion. In *Proceedings of the IEEE/CVF International Conference on Computer Vision*, pages 7452–7461, 2023. 3
- [67] Jinheng Xie, Weijia Mao, Zechen Bai, David Junhao Zhang, Weihao Wang, Kevin Qinghong Lin, Yuchao Gu, Zhijie Chen, Zhenheng Yang, and Mike Zheng Shou. Show-o: One single transformer to unify multimodal understanding and generation. *arXiv preprint arXiv:2408.12528*, 2024. 2
- [68] Jiazheng Xu, Xiao Liu, Yuchen Wu, Yuxuan Tong, Qinkai Li, Ming Ding, Jie Tang, and Yuxiao Dong. Imagereward: Learning and evaluating human preferences for text-to-image generation. In *NeurIPS*, 2023. 6
- [69] Xiaohua Zhai, Basil Mustafa, Alexander Kolesnikov, and Lucas Beyer. Sigmoid loss for language image pre-training. In *Proceedings of the IEEE/CVF international conference on computer vision*, pages 11975–11986, 2023. 3
- [70] Bowen Zhang, Shuyang Gu, Bo Zhang, Jianmin Bao, Dong Chen, Fang Wen, Yong Wang, and Baining Guo. Styleswin: Transformer-based gan for high-resolution image generation. In *Proceedings of the IEEE/CVF Conference on Computer Vision and Pattern Recognition*, pages 11304–11314, 2022. 2
- [71] Hui Zhang, Dexiang Hong, Tingwei Gao, Yitong Wang, Jie Shao, Xinglong Wu, Zuxuan Wu, and Yu-Gang Jiang. Creatilayout: Siamese multimodal diffusion transformer for creative layout-to-image generation. *arXiv preprint arXiv:2412.03859*, 2024. 2, 3, 5, 6, 7
- [72] Kai Zhang, Lingbo Mo, Wenhua Chen, Huan Sun, and Yu Su. Magicbrush: A manually annotated dataset for instruction-guided image editing. In *Advances in Neural Information Processing Systems*, 2023. 3
- [73] Chuayang Zhao, Yuxing Song, Wenhao Wang, Haocheng Feng, Errui Ding, Yifan Song, Xinyan Xiao, and Jingdong Wang. Monoformer: One transformer for both diffusion and autoregression. *arXiv preprint arXiv:2409.16280*, 2024. 2
- [74] Haozhe Zhao, Xiaojuan Shawn Ma, Liang Chen, Shuzheng Si, Rujie Wu, Kaikai An, Peiyu Yu, Minjia Zhang, Qing Li, and Baobao Chang. Ultraedit: Instruction-based fine-grained image editing at scale. *Advances in Neural Information Processing Systems*, 37:3058–3093, 2024. 3
- [75] Chunting Zhou, Lili Yu, Arun Babu, Kushal Tirumala, Michihiro Yasunaga, Leonid Shamis, Jacob Kahn, Xuezhe Ma, Luke Zettlemoyer, and Omer Levy. Transfusion: Predict the next token and diffuse images with one multi-modal model. *arXiv preprint arXiv:2408.11039*, 2024. 2
- [76] Dewei Zhou, You Li, Fan Ma, Xiaoting Zhang, and Yi Yang. Migc: Multi-instance generation controller for text-to-image synthesis. In *CVPR*, 2024. 2, 3, 5, 6

A. Inference Details

We used classifier-free guidance during the inference process of image generation, and the guidance scale is 5. We only apply negative layout guidance when performing layout-guided image manipulation including object deletion. To speed up the inference, we use kv-cache. It takes about 17 seconds to generate 8 images in one batch on a single A100 GPU.

B. Experimental Details

In-context Prompt for Baselines in Layout Planning. Qwen-2.5-7b-instruct and Llama-3.1-8b-instruct themselves do not naturally support the layout planning task. We leverage LLMs’ in-context learning capabilities to generate layouts from global captions following Layout-GPT, and the in-context prompts are as follows:

```
You are an intelligent bounding box generator. I will provide you with a caption for a photo, image, or painting. Your task is to generate the bounding boxes for the objects mentioned in the caption, along with a background prompt describing the scene. The images are of size 512 x512. The top-left corner has coordinate [0, 0]. The bottom-right corner has coordinnate [512, 512]. The bounding boxes should not overlap or go beyond the image boundaries. Each bounding box should be in the format of (object name, [top-left x coordinate, top-left y coordinate, box width, box height]) and should not include more than one object. Do not put objects that are already provided in the bounding boxes into the background prompt. Do not include non-existing or excluded objects in the background prompt. Use "A realistic scene" as the background prompt if no background is given in the prompt. If needed, you can make reasonable guesses. Please refer to the example below for the desired format.
```

```
input: A realistic image of landscape scene depicting a green car parking on the left of a blue truck, with a red air balloon and a bird in the sky
```

```
you need output: [('a green car', [21, 281, 211, 159]), ('a blue truck', [269, 283, 209, 160]), ('a red air balloon', [66, 8, 145, 135]), ('a bird', [296, 42, 143, 100])]
```

```
input: A realistic top-down view of a wooden table with two apples on it
you need output: [('a wooden table', [20, 148, 472, 216]), ('an apple', [150, 226, 100, 100]), ('an apple', [280, 226, 100, 100])]
```

```
input: An oil painting of a pink dolphin jumping on the left of a steam boat on the sea
you need output: [('a steam boat', [232, 225, 257, 149]), ('a jumping pink dolphin', [21, 249, 189, 123])]
```

The input for you to process is: {}

Baselines Details on Image Layout Understanding. For Grounding-DINO, we perform grounding detection by giving the image and the global caption of the image. For two other LLM-based baselines, i.e. CogVLM-grounding and Qwen-VL-Chat, we take prompts suitable for the corresponding models to help the model to output accurate detection results. Specifically, for CogVLM-grounding, we give the image and ask “*Can you provide a description of the image and include the coordinates $[[x_0, y_0, x_1, y_1]]$ for each mentioned object?*” following its formal demo. For Qwen-VL-Chat, we apply two rounds of questions. First, we give the image and ask the model “*What objects are in the image?*”. Then, after the model answers this question, we ask the model “*Box out the positions of these objects in the figure.*”. We find that for Qwen-VL-Chat, the effect of such two-round Q&A will be much better than a single question.

Evaluation of Image Layout Understanding. Similar to HiCo, we calculate the maximum IoU between the boxes predicted by different models and the ground truth boxes. If the maximum IoU is higher than the threshold 0.5, we caculate the clip text similarity between corresponding local descriptions. If the CLIP score is higher than 0.2, we mark it as a correct prediction. We use AR, AP, AP50 and AP75 to evaluate the performance of image layout understanding.

C. Additional Results

We show more examples of layout-guided image manipulation in Figure 8, more examples of layout-image joint generation in Figure 10, more examples of layout-to-image in Figure 11, and more results of image layout understanding in Figure 12. These rich examples show PlanGen’s excel-

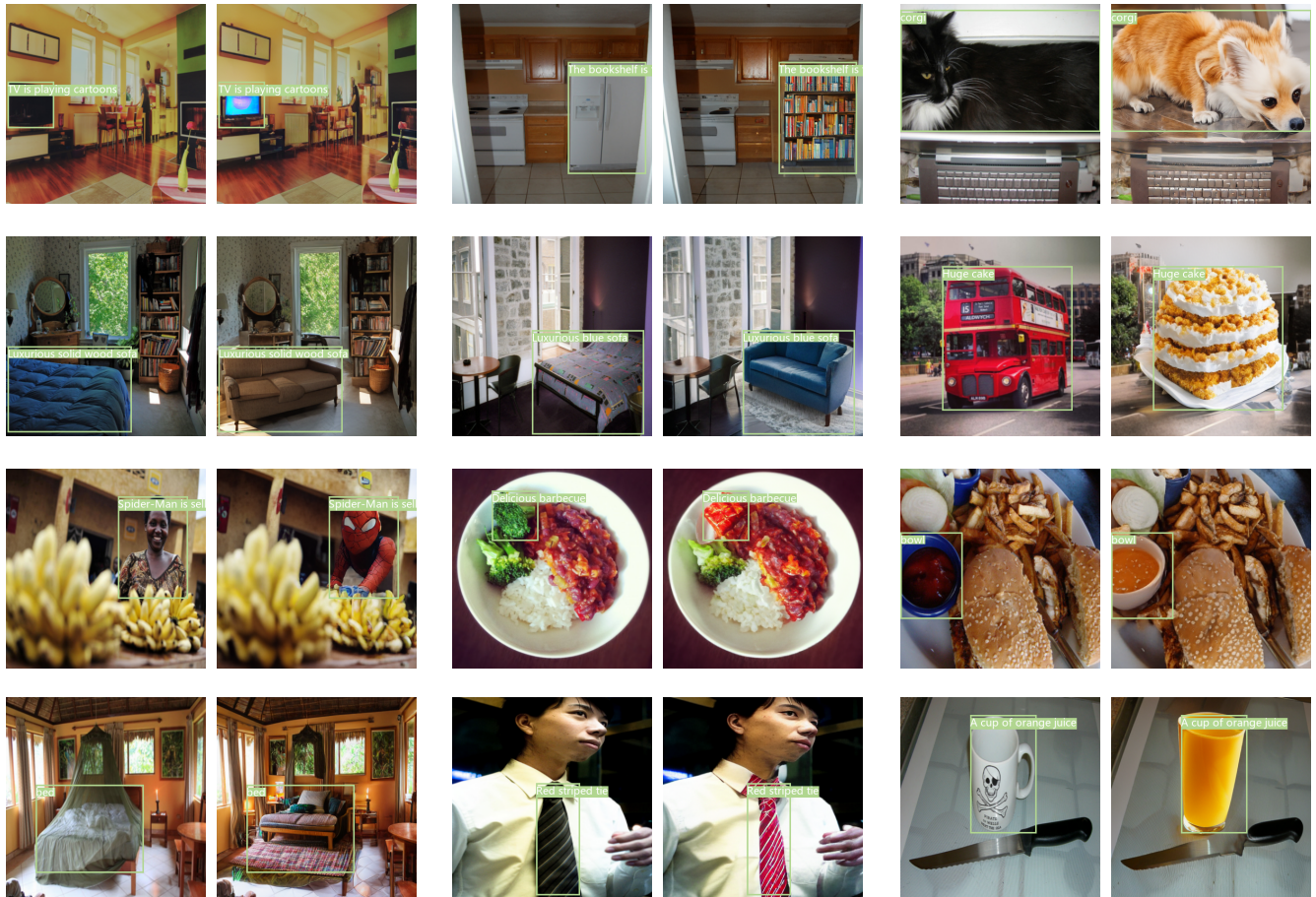


Figure 8. More examples for Layout-guided Image Manipulation. The contents to be edited are drawn in the form of bounding boxes on the original images and the edited images for easy comparisons.

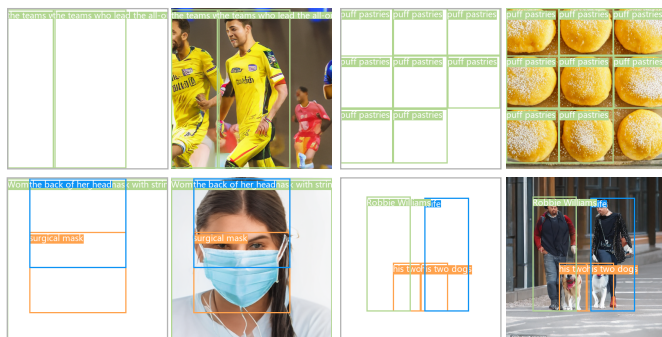
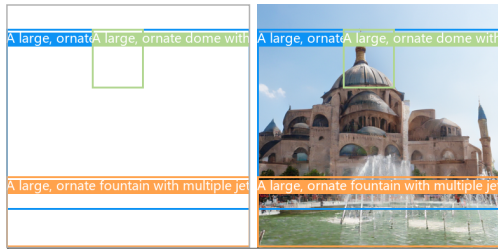


Figure 9. Failure cases.

lent performance on multiple related tasks.

Failure cases. We also show several failure cases on the task of layout-image joint generation in Figure 9. We observed that PlanGen may experience distortion when generating human bodies, as shown in Figure 9, which is a common challenge faced by some previous autoregressive image generation models. When multiple identical objects are generated, additional ones may appear, which is caused

by incomplete object annotations in the training data. In the 2nd row, the the geometry of generated mask straps is slightly inappropriate. When generating dogs in smaller size, the quality declines also occur. More efficient image modeling or wider training should alleviate these problems.



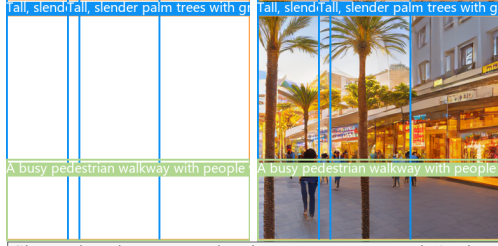
This is a photo showcasing a grand mosque, with its iconic dome and minaret standing out against the blue sky. The mosque is located in a spacious square, surrounded by a fountain with water splashing, and the square is filled with people. The surrounding trees and the blue sky add a touch of natural beauty to this religious building.



This is a photo showcasing fashionable clothing in a store. The focus is on a mannequin dressed in a floral-patterned jacket and a blue scarf, with a plaid-patterned hat on its head. The background is blurred, but other mannequins and clothing can be seen. The entire scene is illuminated by soft indoor lighting, creating a warm shopping atmosphere.



This is a photograph showcasing a city port landscape. In the foreground, a red boat is docked at the pier, with a few people walking on the pier. The midground features a busy harbor with numerous sailboats and yachts moored, and a modern building with a blue roof. The background is a cityscape, with buildings of various styles and sizes, as well as distant hills. The sky is a light blue, with clouds scattered across it.



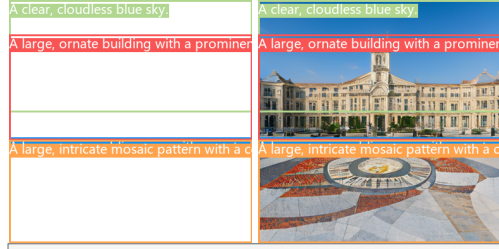
This is a photo showcasing a modern shopping center, capturing the bustling scene of shoppers and the surrounding environment. In the foreground of the photo, there are several tall palm trees, adding a touch of tropical flair to the scene. The center of the photo is a pedestrian walkway, with people walking on it, some carrying shopping bags, others chatting. The shops on both sides of the walkway are brightly lit, displaying various fashionable clothes and accessories. The signboards of the shops are clearly visible, such as 'ALBERTO' and 'MELISSA ODINGA'. The entire scene is illuminated by the soft sunlight, creating a warm shopping atmosphere.



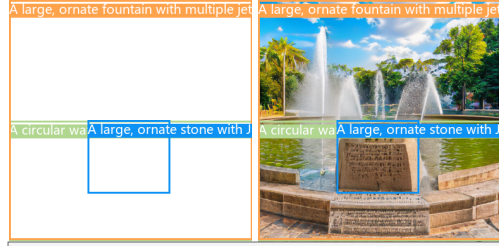
This is a photo showcasing a natural landscape, with a majestic mountain range in the center of the frame, its surface covered with rocks and sparse vegetation. The mountain range is illuminated by sunlight, with the shadows of the peaks clearly visible. In the foreground of the image, there is a small building with a traditional style, its color contrasting with the surrounding environment. The entire scene is captured under clear weather, with a blue sky and a few white clouds, adding a sense of tranquility and vastness to the image.



This is a photo showcasing three stone tablets with Chinese inscriptions. The tablets are arranged in a row, with the one in the middle being the largest, and the two on either side being smaller. Each tablet has a unique design, with the middle tablet having a red background and black Chinese characters, while the two on either side have a yellow background and black Chinese characters. Below the middle tablet is a stone slab with red Chinese characters, and the three tablets are placed on a set of stone steps. The background features some trees and a building, but they are not the focus.



This is a photo showcasing a grand building with a classic European style. The building is located in the center of the picture, with a prominent clock tower at the top, and the facade is decorated with intricate carvings and windows. In front of the building is a spacious square, with a large mosaic pattern in the middle, composed of red, black, and white tiles, and the word 'EUROPA' is written in the middle. The square is paved with white marble, and there are some people and vehicles around. The background is a clear blue sky, with a few white clouds leisurely drifting by.



This is a photograph showcasing a fountain in a park. The fountain is located in the center of the image, with water shooting up from the center, forming a series of elegant arcs. The fountain is surrounded by a circular water pool, with a commemorative stone in the middle. The stone is engraved with Japanese text, which may be the name of the fountain or a commemorative text. The background of the fountain is a lush green park, with a few people walking in the distance. The sky is clear, with a few white clouds scattered across the blue sky.

Figure 10. More examples for Layout-Image Joint Generation. Global captions for layout-image joint generation are attached below the images.

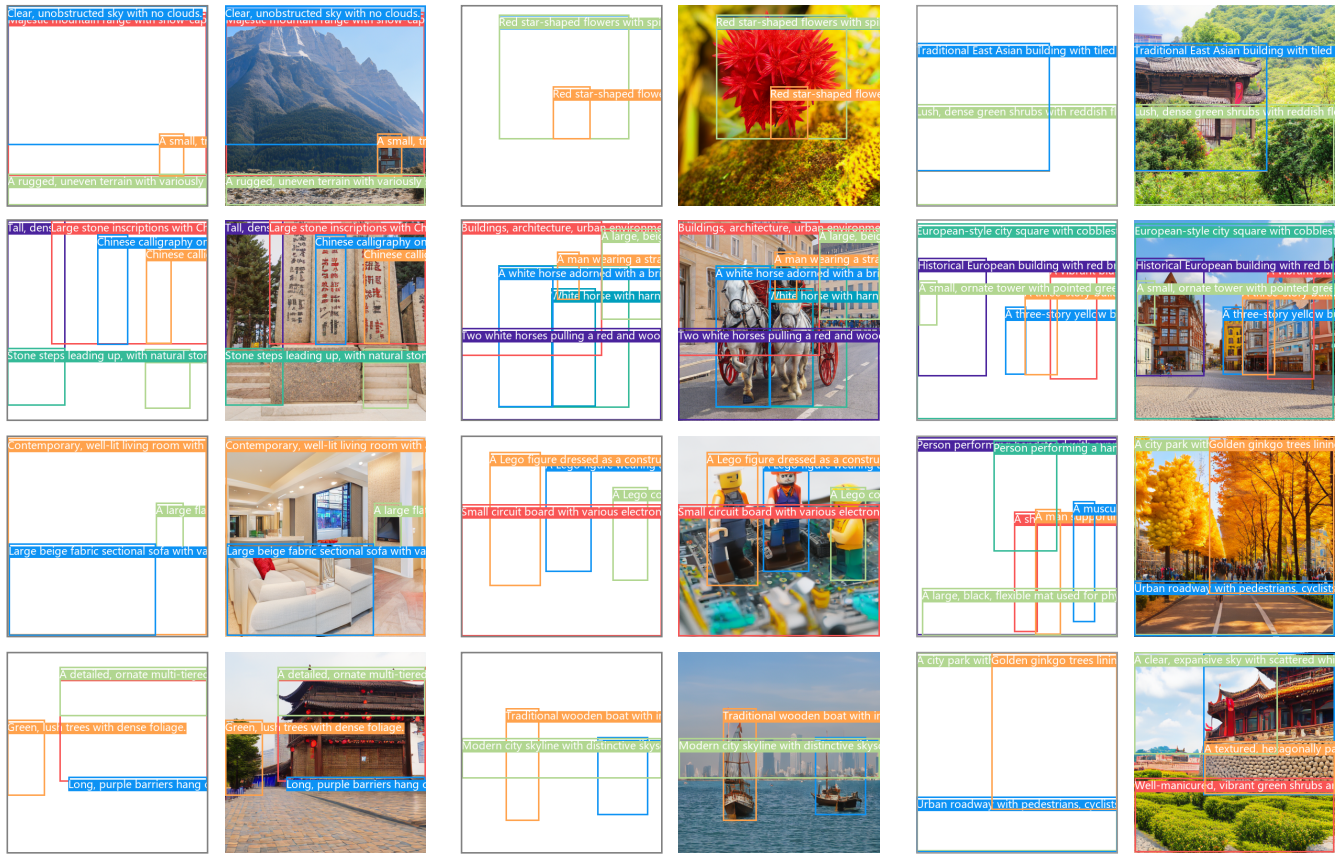


Figure 11. More examples for Layout-to-Image Generation.

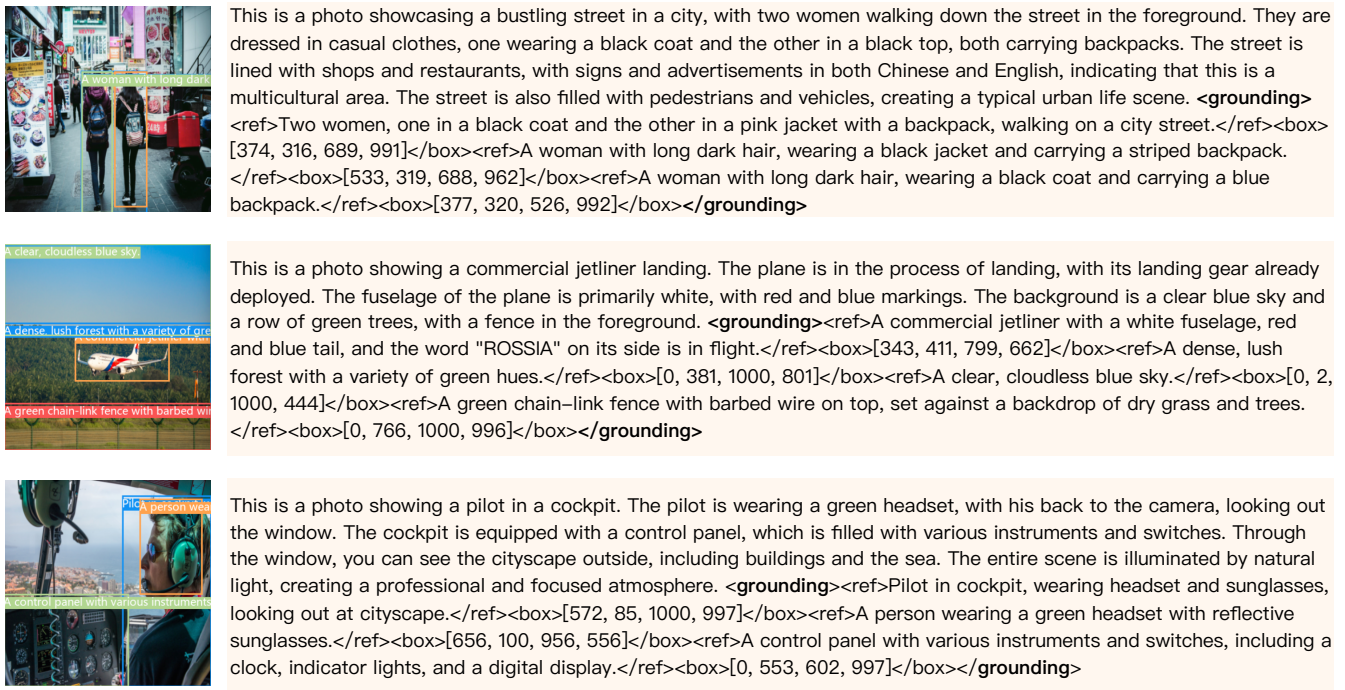


Figure 12. More examples for Image Layout Understanding.